A simple strategy for addition of degron tags to endogenous genes harboring prior insertions of fluorescent protein.

Razan Fakieh[1], Tam Duong[1], You Wu[1], Neal Rasmussen[1], David Reiner[1§]

[1]Texas A&M University

[§]To whom correspondence should be addressed: dreiner@tamu.edu

Abstract

There exist insufficient validated "entry portal" sites in the *C. elegans* genome for CRISPR/Cas9-dependent insertion into endogenous genes to confer diverse spatiotemporal patterns and levels of expression on exogenous sequences. Consequently, we recognized the most common potential "entry portal" sequences: genes previously tagged with fluorescent proteins using CRISPR/Cas9. As proof of concept, we used existing mKate2-encoding sequences inserted in the 5' end of genes as an insertion point for the auxin inducible degron, AID*. This sequence permits reasonably efficient insertion that can be employed using a variety of approaches for different end goals. Our strategy is thus generalizable to many needs.
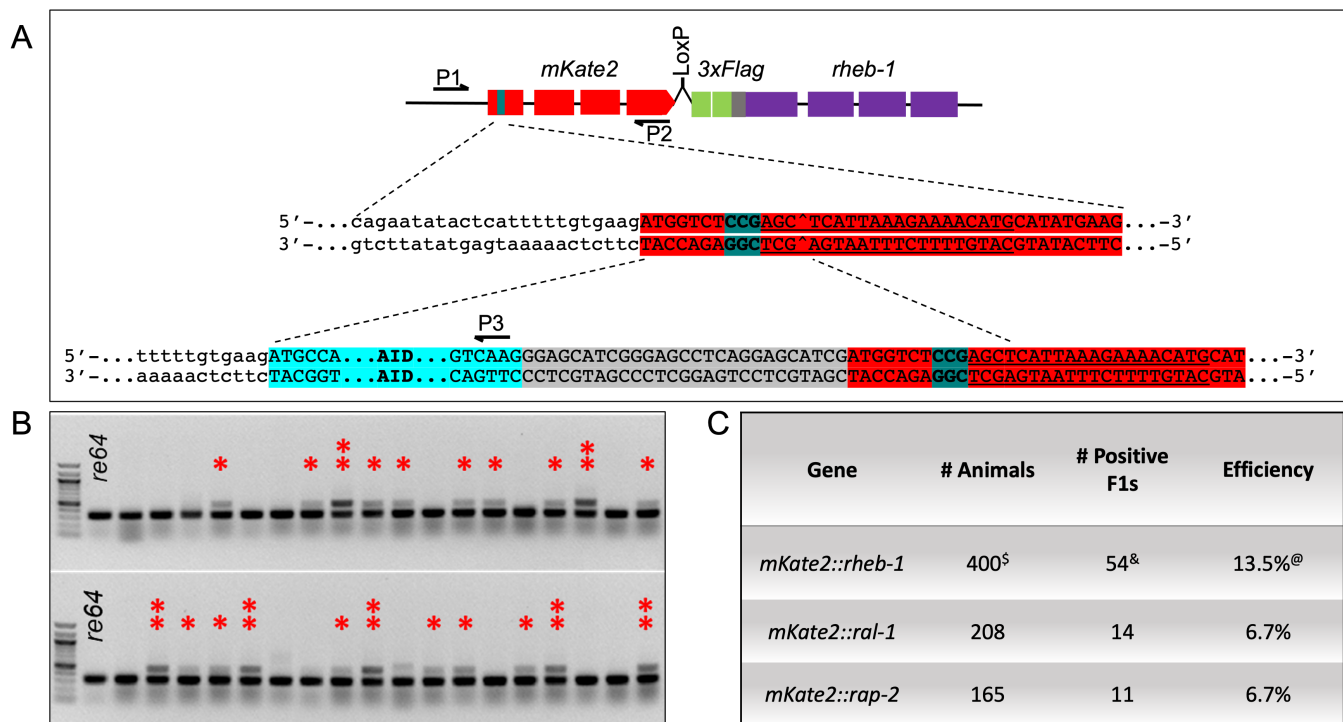
Figure 1. Insertion of AID* into the 5' end of *mKate2*.

A) A schematic of AID* insertion into *mKate2::3xFlag::rheb-1*. Red depicts sequences encoding mKate2, cyan depicts sequences encoding AID*, teal indicates PAM sequences on the reverse strand, underlining indicates the guide RNA on the reverse strand with the carat symbol indicating the cut site, green depicts sequences encoding 3xFlag, gray depicts sequences encoding linker, and purple depicts the *rheb-1* gene. P1, P2 and P3 indicate locations of triplex PCR detection primers. **B)** The agarose gel for genotyping AID* insertion into *mKate*-tagged *rheb-1*. *re64* is the original *mKate2::3xFlag::rheb-1* strain, which yields a 337 bp band. AID* insertion bands are at 499 bp. Pools of four F1 animals were on each plate and in each PCR tube. One asterisk indicates a likely insertion event in one of the eight homologous chromosomes present in the pool of four co-CRISPRed F1 animals. The two vertical asterisks marking darker insertion bands indicate likely insertion events in two or more chromosomes, either as a homozygous insertion or heterozygous in two different animals. Pools of four were only used for insertion into *mKate2::3xFlag::rheb-1*. **C)** Table portraying efficiency of insertion. For each *mK2::gene*, the number of Rol animals picked, number of positive F1 candidates and efficiency rate for each gene are shown. [$] Total number of animals picked in pools of 4, equaling 100 reaction/400 F1 animals. [&] Estimate of positive F1 candidates from *mK2::rheb-1* pools. [@] Estimate of the efficiency rate for AID insertion into *mKate2::3xFlag::rheb-1*.

Description

Genome editing with CRISPR in association with the bacterial nuclease Cas9 ("CRISPR/Cas9") is used experimentally in many organisms and is under development for therapeutic applications. CRISPR has been applied successfully in *C. elegans* in a wide variety of contexts, from simple gene knockouts and knockins of missense and nonsense mutations to more elaborate tagging of genes, chromosomal rearrangements and constructs for a wide variety of applications, (*e.g.* Ashley et al., 2021; Dejima et al., 2018; Dickinson et al., 2015; Dickinson et al., 2013; Friedland et al., 2013). Additionally, over the recent years various improvements in efficiency of CRISPR workflows have improved the potential for *a la carte* editing of the *C. elegans* genome (Arribere et al., 2014; Dokshin et al., 2018; Ghanta & Mello, 2020; Kim et al., 2014; Paix et al., 2015; Paix et al., 2016; Paix et al., 2014). Yet efficiency is still determined in part by selection of the 20 nt target sequences immediately upstream of the PAM (protospacer adjacent motif) for recognition by the Cas9 ribonucleoprotein complex. Selection of this target sequence during the design phase of an editing project determines synthesis of CRISPR RNAs (crRNAs or "guides") for subsequent edits.

However, there persists great variability in efficiency of cutting, for example due to position in the gene or local chromatin context in the tissue in which cutting occurs (Chen et al., 2017; Ghanta & Mello, 2020; Horlbeck et al., 2016; Strohkendl et al., 2021; Yarrington et al., 2018), *i.e.* the distal gonad in *C. elegans*. These variables can reduce efficiency of editing projects or even prevent successful editing. One solution for this problem is to use validated "entry portals" for inserting large sequences. These sites could be either introduced exogenously into the *C. elegans* genome or using defined endogenous sequences previously demonstrated to be effective for insertions (Silva-Garcia et al., 2019; Stevenson et al., 2020). Alternatively, one could use "entry portal" sites serendipitously generated as part of CRISPR insertion projects for other ends, such as tagging endogenous genes with sequences encoding fluorescent proteins (FPs), epitopes for detection by antibodies, or other manipulations.

We identified the 5' end of sequences encoding the mKate2 red fluorescent protein, used to tag endogenous genes to track proteins visually, as such a potential "entry portal" sequence to be used frequently for other applications (see Methods). Our lab has generated tags of three independent genes at the 5' end with germline optimized (GLO; Fielmich et al., 2018) *mKate2*-encoding sequences. We have identified a guide RNA site in the 5' end of the *mKate2* sequence that facilitates efficient insertion of desired sequences. We then used this site to insert a chemical genetic tool, the conditional auxin inducible degron (AID*; Zhang et al., 2015), into *mKate2* sequences already present in the genome. These sites mediate insertion at levels of efficiency likely to support generalized use of *mKate2* insertions as entry portals for editing into any gene previously modified by insertion of sequences encoding mKate2.

Specifically, we edited the 5' ends of endogenous genes *ral-1*, *rheb-1* and *rap-2*, all of which encode small GTPases of the Ras family. All three had sequences encoding *mKate2^3xFlag* inserted at the 5' end (Duong et al., 2020; Shin et al., 2018; Fakieh and Reiner unpublished results) using the SEC approach (Dickinson et al., 2015). We identified a possible guide sequence near the 5' end of *mKate2* as a candidate insertion site (**Fig. 1A**). Using PCR oligonucleotides with homology arms matching the surrounding *mKate2* sequences, we PCR amplified *AID** sequences from plasmid pBS::AID::mkate2::2xHA::AID* (see Methods). This amplicon was used to repair into the endogenous *mKate2*-inserted locus cut with Cas9 (see Methods). Successful editing into this targeted site resulted in *AID** insertion into *mKate2^3xFlag::rheb-1* with substantial efficiency: conservatively, ~13.5% of *mKate2::rheb-1* animals had AID* insertions in the candidate site at the 5' end of *mKate::3xFlag* sequence inserted in *rheb-1* (**Fig. 1B**). AID* was inserted into *mKate2^3xFlag::ral-1* and *mKate2^3xFlag::rap-2* with 6.7% efficiency rate for both (**Fig. 1C**).

The *rheb-1* and *ral-1* genes are essential for *C. elegans* development. The originally characterized mKate2-tagged insertions for these two genes were validated by Western blot and assessment of function (Duong et al., 2020; Shin et al., 2018). *rap-2*, in contrast, is not essential for viability (Pellis-van Berkel et al., 2005). Thus, the *mKate::3xFlag* tag into *rap-2* has not been validated functionally. For all three genes, the proper insertion of AID* was confirmed by sequencing regions that had undergone homology-directed repair (HDR).

From this study we can extrapolate that efficiency of insertion in this mKate2 site is high enough to be used for introduction of desired sequences into the 5' end of sequences encoding *mKate2* in diverse loci in the genome. We demonstrated proof of concept with insertion of *AID**, but the approach can be generalized to other edits in the genome.

Diverse future applications follow from this observation. First, development of similar sites in the of 3' sequences in *mKate2*-encoding sequences would facility for similar editing but at genes with *mKate2*-encoding sequences inserted at their 3' ends, to keep inserted sequences distal from the native gene. Identification and validation at similar sites of other FPs, like eGFP, mNeonGreen, mTurquoise, mScarlet, etc., both at 5' and 3' ends, would maximize the potential for insertion at diverse points in the genome. Furthermore, selection of previously tagged genes with defined but limited expression patterns would facilitate expression of inserted sequences in those same limited tissues, particularly if the user employs 2A-related ribosomal skip

peptides for independent protein expression from the same locus (Ahier & Jarriault, 2014). Similarly, genes with previously defined differences in expression levels could be tagged and used as insertion points, which could confer similar control on independent exogenous sequences inserted at the locus. For example, while in some cases, like heat shock-dependent expression (Russnak & Candido, 1985), extremely high protein levels might be desirable, often physiologically relevant gene expression might be more desirable and demands can vary by experiment. These approaches would be limited only by the availability and characterization of previously tagged genes, but the size of this list is increasing exponentially.

In summary, we defined an efficient insertion site via CRISPR in the 5' end of *mKate2*-encoding sequences inserted into endogenous genes. We demonstrated successful insertions of AID*-encoding sequences into the 5' ends of three genes, *rheb-1*, *ral-1* and *rap-2*. This efficiency establishes feasibility for additional edits in different parts of the genome. With sufficiently high efficiency, researchers should be reasonably confident of inserting any sequence desired. Additionally, this method will facilitate the use of diverse endogenous promoters in the animal, imposing a variety of conditions for heterologous expression.

Methods

Strains: Strains were grown with OP50 bacteria on NGM agar plates at 20°C unless otherwise stated. All strains used in this study are listed in (**Table 1**) and primers in (**Table 2**).

Selection of guide RNA sequence. The variability of the guide selection process was mitigated using certain general principles. First, we used a combination of algorithms at CRISPOR (http://crispor.tefor.net/) and WU-CRISPR (http://crisprdb.org/wu-crispr/) to evaluate potential guide RNAs and their uniqueness in the *C. elegans* genome (Doench et al., 2016; Wong et al., 2015). Second, in general we favor use of a "GG" dinucleotide at positions -1 and -2 upstream of the PAM (Farboud & Meyer, 2015), but that requirement was not met for the guide RNA used in this study and efficiency was still reasonable.

Preparation of repair template: AID* repair template was amplified by PCR from plasmid pBS::AID*::mKate2::2xHA::AID with germline optimized sequences (Neal Rasmussen, personal communication, DNA sequence available upon request). PCR primers had 5' end homology arms matching sequences flanking the Cas9 cut site in *mKate2* to facilitate HDR (**Table 2**). The resulting PCR products were evaluated by gel electrophoresis and column purified using the Invitrogen PCR Purification Kit. Resulting purified repair template was added to the injection mix at the appropriate concentration (see below).

Preparing components for CRISPR: The composition of the injection mix was derived from a number of previous publications (Dokshin et al., 2018; Paix et al., 2015; Paix et al., 2016; Paix et al., 2014). The injection mix is presented in tabular form, below, and is assembled as two separate mixes, the Cas9/RNA complex and the DNA repair mix. All reported final concentrations are in reference to the final combined 20 µl injection mix.

	Injection Mix	Final Conc. - Injection Mix (20 µl)	
Cas9	1 µl of 5 µg/µl	0.25 µg/µl	
tracrRNA	1 µl of 2 µg/µl	0.1 µg/µl	Incubate at 37°C for 15 min
dpy-10 crRNA	1.4 µl of 0.4 µg/µl	0.028 µg/µl	
gene-specific crRNA	1.4 µl of 0.4 µg/µl	0.028 µg/µl	

dpy-10 ssODN repair	3.3 µl from 20 µM	3.3 µM = 2 µg = 100 ng/µl	
gene-specific ssODN repair	6.6 µl from 10 µM	3.3 µM = ? µg = ? ng/µl	
or			

gene-specific PCR product repair	2 µg	100 ng/µl	Incubate according to Mello Donor PCR stepdown below
ddH20	up to 20 µl	----------	

Do not add PCR repair template to RNP mix until Mello donor program has been run

To identify animals in which CRISPR editing had occurred in a gamete from the parents, we used the *dpy-10(cn64*gf*)* semi-dominant co-CRISPR marker phenotype, with repair template co-injected as a single-stranded DNA oligonucleotide (Arribere et al., 2014). Independently of the enzyme mix, repair template for *AID** insertion was made using two different protocols. First, for insertion into *mKate2::3xFlag::rheb-1*, two PCR templates of *AID** were amplified, with and without homology arms matching flanking *mKate2* sequences. The two PCR products were mixed at 0.4 µg/ml and subjected to a melting-annealing program to facilitate formation of "bubbles" due to incomplete reannealing (Ghanta et al., 2021; Ghanta & Mello, 2020). The program was as described (Ghanta et al., 2021): 95˚C 2:00 min; 85˚C 10 sec.; 75˚C 10 sec, 65˚C 10 sec, 55˚C 1:00 min, 45˚C 30 sec, 35˚C 10 sec, 25˚C 10 sec, with ramp down increments of 1˚C/sec, then held at 4˚C.

Second, for insertion into *mKate2::3xFlag::ral-1* and *mKate2::3xFlag::rap-2,* we amplified *AID** with homology arms, without the added step of generating a heteroduplex from two different PCR products. For this second approach, 3.3 µM final concentration of the *AID** PCR product was subjected to the same melting-annealing program described above.

For both approaches, 3.3 µM final concentration of *dpy- 10* single-stranded oligonucleotide repair template was added to the PCR product, the final 15.2 µl in nuclease free water, added to the 4.8 µl of ribonucleoprotein complex for a final volume of 20 µl and very gently mixed without vortexing. This mix was filtered through a 0.45 µm cutoff ultrafiltration spin-columns (EMD Millipore Corp.) for 2 minutes at 13,000 rpm.

Injection and isolation: We injected mid-adult animals with no greater than one row of embryos in the uterus. P_{inj} animals were picked singly to spotted plates and incubated at 20 °C for ~96 hrs. The oldest F1 animals, corresponding roughly to the first 24 hrs of egg laying, were passed over. From the younger cohort of F1s, we picked animals expressing the Rol co-CRISPR marker singly to plates, with the exception of *rheb-1*, which were picked in pools of four. The next day, parents were picked into tubes and lysed for single-worm PCR with triplex detection primers (Table 2). PCR products were run on 2% agarose gels. Homozygotes segregated from positive F1 parents were isolated from singly cloned F2 non-Rol animals, then tested and confirmed by PCR.

Reagents

Table 1: List of Strains used in this study

Strain	Genotype
DV3066	*rheb-1(re64[mKate2^3xFlag::rheb-1]) III*
DV3668	*rheb-1(re64 re283[AID*::mKate2^3xFlag::rheb-1]) III*
DV3402	*ral-1(re218[mKate2^3xFlag::ral-1]) III*
DV3814	*ral-1(re218 re319[AID*::mKate2^3xFlag::ral-1]) III*
DV4012	*rap-2(re346[mKate2^3xFlag::rap-2]) V*
DV4021	*rap-2(re346 re355[AID*::mKate2^3xFlag::rap-2]) V*

Table 2: List of DNA and RNA oligonucleotides used in this study

Name	Description	Sequence[a]
tracrRNA	tracer RNA	AACAGCAUAGCAAGUUAAAAUAAGGCUAGUCCGUUAUCAACUUGAAAAAGUGGCACCGAGUCGGUGCUUUUUUU
TD332	*mKate2* crRNA	CAUGUUUUCUUUAAUGAGCUCGG + GUUUUAGAGCUAUGCUGUUUUG
dpy-10	*dpy-10* crRNA	GCUACCAUAGGCACCACGAG + GUUUUAGAGCUAUGCUGUUUUG
dpy-10 rep	Repair template for *dpy-10* co-CRISPR	CACTTGAACTTCAATACGGCAAGATGAGAATGACTGGAAACCGTACCGCATGCGGTGCCTATGGTAGCGGAGCTTCACATGGCTTCAGACCAACAGCCTAT
TD326	*AID**(for) repair template in *rheb-1* with homology arm	tcaatcattcaatattcagaatatactcatttttgtgaagATG CCAAAGGACCCAGCTAA
TD327	*AID**(rev) universal repair template with homology arm in *mKate2*[b]	CCCTCCATGTAGAGCTTCATATGCATGTTTTCTTTAATGAGCTCGGAGACCATCGATGCTCCTGAGG
TD328	*AID**(for) repair template without homology arm	ATGCCAAAGGACCCAGCTAA
TD329	*AID**(rev) repair template without homology arm	ACCATCGATGCTCCTGAGG
TD330	genotyping (for) *rheb-1*	gcgcatattattgcaaaagtacatc
TD331	genotyping (rev) (in *mKate2*)[c]	CCTCGACGGCCTTGATAC
YW10	*AID**(for) repair template in *ral-1* with homology arm	tttcccccgggttttccccctaaaactcgaattttcagccATG CCAAAGGACCCAGCTAAG
YW11	genotyping (for) *ral-1* in promoter	tcagaatggagggttacggt
YW59	genotyping (for) *ral-1* in AID*	GCCACCAGTTCGTTCTTACC
RF89	*AID**(for) repair template with *rap-2* homology arm	cacctaatccaatttattgattttcagcaaaaaactctca ATGCCAAAGGACCCAGCTAA
RF91	genotyping (for) *rap-2* in promoter	gctactccactttagaatcaatttcagc
RF92	genotyping (rev) *rap-2* in AID*	CGGTAAGAACGAACTGGTGGC

RF93	genotyping (rev) *rap-2* in *mKate2*	GCGAATGGGAGTGGTCCTC

[a]For primers for PCR of repair templates, seed primers are underlined and the chimeric sequences of homology arms not underlined

[b]This reverse primer is universal for all insertions at this locus because the seed primer recognizes *AID** and the homology arm is in *mKate2*. Because repairs neighbor promoter sequences at the 5' end, a different homology arm will be needed for each 5' forward primer for amplification of *AID**.

[c]For *AID** insertion into *mKate2::3xFlag::rheb-1* only two detection primers were used, flanking AID* in the *rheb-1* promoter and in *mKate2*. But TD331(rev) was also used in triplex PCR to detect insertions into *mKate2::3xFlag::ral-1* and could theoretically be used for other insertions into *mKate2*-encoding sequences.

References

Ahier A, Jarriault S. 2014. Simultaneous expression of multiple proteins under a single promoter in Caenorhabditis elegans via a versatile 2A-based toolkit. Genetics 196: 605-13. PubMed ID: 24361941

Arribere JA, Bell RT, Fu BX, Artiles KL, Hartman PS, Fire AZ. 2014. Efficient marker-free recovery of custom genetic modifications with CRISPR/Cas9 in Caenorhabditis elegans. Genetics 198: 837-46. PubMed ID: 25161212

Ashley GE, Duong T, Levenson MT, Martinez MAQ, Johnson LC, Hibshman JD, et al., Ward JD. 2021. An expanded auxin-inducible degron toolkit for Caenorhabditis elegans. Genetics 217: . PubMed ID: 33677541

Chen X, Liu J, Janssen JM, Gonçalves MAFV. 2017. The Chromatin Structure Differentially Impacts High-Specificity CRISPR-Cas9 Nuclease Strategies. Mol Ther Nucleic Acids 8: 558-563. PubMed ID: 28918055

Dejima K, Hori S, Iwata S, Suehiro Y, Yoshina S, Motohashi T, Mitani S. 2018. An Aneuploidy-Free and Structurally Defined Balancer Chromosome Toolkit for Caenorhabditis elegans. Cell Rep 22: 232-241. PubMed ID: 29298424

Dickinson DJ, Pani AM, Heppert JK, Higgins CD, Goldstein B. 2015. Streamlined Genome Engineering with a Self-Excising Drug Selection Cassette. Genetics 200: 1035-49. PubMed ID: 26044593

Dickinson DJ, Ward JD, Reiner DJ, Goldstein B. 2013. Engineering the Caenorhabditis elegans genome using Cas9-triggered homologous recombination. Nat Methods 10: 1028-34. PubMed ID: 23995389

Doench JG, Fusi N, Sullender M, Hegde M, Vaimberg EW, Donovan KF, et al., Root DE. 2016. Optimized sgRNA design to maximize activity and minimize off-target effects of CRISPR-Cas9. Nat Biotechnol 34: 184-191. PubMed ID: 26780180

Dokshin GA, Ghanta KS, Piscopo KM, Mello CC. 2018. Robust Genome Editing with Short Single-Stranded and Long, Partially Single-Stranded DNA Donors in *Caenorhabditis elegans*. Genetics 210: 781-787. PubMed ID: 30213854

Duong T, Rasmussen NR, Ballato E, Mote FS, Reiner DJ. 2020. The Rheb-TORC1 signaling axis functions as a developmental checkpoint. Development 147: . PubMed ID: 32041790

Farboud B, Meyer BJ. 2015. Dramatic enhancement of genome editing by CRISPR/Cas9 through improved guide RNA design. Genetics 199: 959-71. PubMed ID: 25695951

Fielmich LE, Schmidt R, Dickinson DJ, Goldstein B, Akhmanova A, van den Heuvel S. 2018. Optogenetic dissection of mitotic spindle positioning in vivo. Elife 7: . PubMed ID: 30109984

Friedland AE, Tzur YB, Esvelt KM, Colaiácovo MP, Church GM, Calarco JA. 2013. Heritable genome editing in C. elegans via a CRISPR-Cas9 system. Nat Methods 10: 741-3. PubMed ID: 23817069

Ghanta KS, Ishidate T, Mello CC. 2021. Microinjection for precision genome editing in *Caenorhabditis elegans*. STAR Protoc 2: 100748. PubMed ID: 34505086

Ghanta KS, Mello CC. 2020. Melting dsDNA Donor Molecules Greatly Improves Precision Genome Editing in *Caenorhabditis elegans*. Genetics 216: 643-650. PubMed ID: 32963112

Horlbeck MA, Witkowsky LB, Guglielmi B, Replogle JM, Gilbert LA, Villalta JE, et al., Weissman JS. 2016. Nucleosomes impede Cas9 access to DNA in vivo and in vitro. Elife 5: . PubMed ID: 26987018

Kim H, Ishidate T, Ghanta KS, Seth M, Conte D Jr, Shirayama M, Mello CC. 2014. A co-CRISPR strategy for efficient genome editing in Caenorhabditis elegans. Genetics 197: 1069-80. PubMed ID: 24879462

Paix A, Folkmann A, Rasoloson D, Seydoux G. 2015. High Efficiency, Homology-Directed Genome Editing in Caenorhabditis elegans Using CRISPR-Cas9 Ribonucleoprotein Complexes. Genetics 201: 47-54. PubMed ID: 26187122

Paix A, Schmidt H, Seydoux G. 2016. Cas9-assisted recombineering in C. elegans: genome editing using in vivo assembly of linear DNAs. Nucleic Acids Res 44: e128. PubMed ID: 27257074

Paix A, Wang Y, Smith HE, Lee CY, Calidas D, Lu T, et al., Seydoux G. 2014. Scalable and versatile genome editing using linear DNAs with microhomology to Cas9 Sites in Caenorhabditis elegans. Genetics 198: 1347-56. PubMed ID: 25249454

Pellis-van Berkel W, Verheijen MH, Cuppen E, Asahina M, de Rooij J, Jansen G, et al., Zwartkruis FJ. 2005. Requirement of the Caenorhabditis elegans RapGEF pxf-1 and rap-1 for epithelial integrity. Mol Biol Cell 16: 106-16. PubMed ID: 15525675

Russnak RH, Candido EP. 1985. Locus encoding a family of small heat shock genes in Caenorhabditis elegans: two genes duplicated to form a 3.8-kilobase inverted repeat. Mol Cell Biol 5: 1268-78. PubMed ID: 4033652

Shin H, Kaplan REW, Duong T, Fakieh R, Reiner DJ. 2018. Ral Signals through a MAP4 Kinase-p38 MAP Kinase Cascade in C. elegans Cell Fate Patterning. Cell Rep 24: 2669-2681.e5. PubMed ID: 30184501

Silva-García CG, Lanjuin A, Heintz C, Dutta S, Clark NM, Mair WB. 2019. Single-Copy Knock-In Loci for Defined Gene Expression in *Caenorhabditis elegans*. G3 (Bethesda) 9: 2195-2198. PubMed ID: 31064766

Stevenson ZC, Moerdyk-Schauwecker MJ, Jamison B, Phillips PC. 2020. Rapid Self-Selecting and Clone-Free Integration of Transgenes into Engineered CRISPR Safe Harbor Locations in *Caenorhabditis elegans*. G3 (Bethesda) 10: 3775-3782. PubMed ID: 32816924

Strohkendl I, Saifuddin FA, Gibson BA, Rosen MK, Russell R, Finkelstein IJ. 2021. Inhibition of CRISPR-Cas12a DNA targeting by nucleosomes and chromatin. Sci Adv 7: . PubMed ID: 33692102

Wang T, Wei JJ, Sabatini DM, Lander ES. 2014. Genetic screens in human cells using the CRISPR-Cas9 system. Science 343: 80-4. PubMed ID: 24336569

Wong N, Liu W, Wang X. 2015. WU-CRISPR: characteristics of functional guide RNAs for the CRISPR/Cas9 system. Genome Biol 16: 218. PubMed ID: 26521937

Yarrington RM, Verma S, Schwartz S, Trautman JK, Carroll D. 2018. Nucleosomes inhibit target cleavage by CRISPR-Cas9 in vivo. Proc Natl Acad Sci U S A 115: 9351-9358. PubMed ID: 30201707

Zhang L, Ward JD, Cheng Z, Dernburg AF. 2015. The auxin-inducible degradation (AID) system enables versatile conditional protein depletion in C. elegans. Development 142: 4374-84. PubMed ID: 26552885